JOURNAL OF COMPUTATIONAL PHYSICS 55, 115–128 (1984)

Chebyshev 3-D Spectral and 2-D Pseudospectral Solvers for the Helmholtz Equation

P. HALDENWANG*, G. LABROSSE*, AND S. ABBOUDI*

Département d'Héliophysique, Université de Provence, Centre de Saint-Jérôme, Marseille, France

AND

M. DEVILLE

Unité de Mécanique Appliquée, Université Catholique de Louvain, Louvain-la-Neuve, Belgium

Received March 3, 1983; revised July 19, 1983

Two Chebyshev solvers are presented for the linear Helmholtz equation. The first algorithm is a 3 D direct spectral solver based on a diagonalization technique, whilst the second performs an iterative pseudospectral 2-D calculation with finite difference preconditioning. Both techniques handle general nonhomogeneous boundary conditions. Computing times and accuracies of the two methods are compared.

1. INTRODUCTION

This paper is concerned with two Chebyshev Helmholtz solvers. The first one is a direct spectral solver derived from the algorithm proposed by Haidvogel and Zang (hereafter referred to as HZ) [2], which has been extended to include the 3-D case and general nonhomogeneous linear boundary conditions. The second solver is an extension of the iterative method proposed by Orszag [5] to 1-D and 2-D general Helmholtz resolution, employing Chebyshev schemes.

Section 2 presents the direct solver for general nonhomogenous boundary conditions (Dirichlet, Neumann or Robbins). The algorithm performs a full diagonalization of the global system matrix or a partial diagonalization associated with the solution of quasi-tridiagonal systems.

Section 3 describes the extension to the Chebyshev case of the analysis presented in [5] for the Fourier case and reports numerical results.

Section 4 compares both algorithms from the point of view of computing time and accuracy.

It is shown that for a Helmholtz equation with constant coefficients, the method

* Equipe de Recherche Associéee CNRS No. 538.

0021-9991/84 $3.00

utilizing full diagonalization is as successful as the Haidvogel–Zang algorithm, while for more general elliptic operations, the pseudospectral scheme leads to spectral accuracy but with significant computing cost.

2. Direct Spectral Solver

This section presents the 3-D fast spectral solver based on a diagonalization technique for general nonhomogeneous boundary conditions. For the sake of simplicity, we will restrict the presentation of basic concepts to the one-dimensional differential equation,

$$u_{xx} - au = f, \qquad x \in [-1, +1], \tag{1}$$

where u_{xx} denotes the second-order derivative of u with respect to x and $a > 0$. To solve Eq. (1), the following boundary conditions are imposed:

$$\alpha_{\pm} u + \beta_{\pm} u_x = g_{\pm}, \qquad \text{at} \quad x = \pm 1. \tag{2}$$

Looking for the solution of (1)–(2) and using the Chebyshev approximation of u,

$$u_N = \sum_{n=0}^{N} \tilde{u}_n T_n(x),$$

the Tau projection method [1] leads to the linear system

$$\tilde{u}_n^{(2)} - a\tilde{u}_n = \tilde{f}_n, \qquad 0 \leqslant n \leqslant N-2, \tag{3}$$

$$\sum_{n=0}^{N} (\pm 1)^n [\alpha_{\pm} \pm \beta_{\pm} n^2] \tilde{u}_n = g_{\pm}, \tag{4}$$

where $\tilde{f}_n$ are the Chebyshev modes of the right-hand side of (1) and $\tilde{u}_n^{(2)}$ denote the coefficients of the second-order derivative (see (A.1)).

The extension of the diagonalization technique proposed by Haidvogel and Zang [2] to the case of nonhomogeneous boundary conditions is based on the reduction of system (3)–(4) of order $(N+1)$ to a system of order $(N-1)$ by algebraic elimination of Eqs. (4). We refer the reader to Appendix I for details of the algebra. The new resulting system is $(B_x - aI)\tilde{u} = D$ (A.5).

The algorithm then proceeds to the calculation of the eigenvalues and eigenvectors of the B_x matrix. Denoting by H_x and Λ_x the matrices formed by the eigenvectors and eigenvalues of B_x, respectively, (A.5) is equivalent to

$$H_x(\Lambda_x - aI) H_x^{-1} \tilde{u} = D. \tag{5}$$

This equation is solved directly, first for $(H_x^{-1}\tilde{u})$, in the eigenvectorspace, and then for $\tilde{u}$ in the $(N-1)$ subspace $\{\tilde{u}_n, n = 0, \ldots, N-2\}$. The last two components

TABLE I

$(N^4, (N-1)^4)$ Law of the Last $(\lambda_k, \lambda_{k-1})$ Eigenvalues

k	Dirichlet case	Neumann case
N	−0.303	−0.474 $E-01$
$N-2$	−0.163 $E-01$	−0.823 $E-02$
$N-4$	−0.502 $E-02$	−0.338 $E-02$
$N-6$	−0.242 $E-02$	−0.182 $E-02$
$N-8$	−0.142 $E-02$	−0.115 $E-02$

$(\tilde{u}_{N-1}, \tilde{u}_N)$ are deduced, from (A.3), (A.4), by taking the boundary conditions into account.

The diagonalization technique works successfully because all eigenvalues are distinct, real and negative (see Gottlieb and Lustman [3]). From numerical experiments, one observes that the smallest eigenvalues behave as in the Fourier case, provided the cutoff of the spectral series is large enough to allow a good representation of the corresponding low-frequency Fourier eigenvectors. Above a value close to $2N/3$, the Chebyshev eigenvalues deviate significantly from the eigenvalues given by the Fourier representation: starting from the last eigenvalue λ_N, the pairs $(\lambda_k, \lambda_{k-1})$ with $k = N, N-2, \ldots$ show, respectively, an identical $(N^4, (N-1)^4)$ law, which is independent of N (see Table I).

For the case of a Poisson's equation ($a = 0$) with Neumann boundary conditions, the RHS of system (3)–(4) must verify the following compatibility condition,

$$\sum_{\substack{n=0 \\ n \text{ even}}}^{N-2} \frac{-2}{n^2-1} \tilde{f}_n = g_+ - g_-, \tag{6}$$

which is none other than the Tau representation of the Cauchy–Neumann condition

$$\int_{-1}^{1} f\,dx = u_x(1) - u_x(-1).$$

For 2-D or 3-D problems, the above procedure can be applied in a straightforward manner to provide a full or partially diagonalized algorithm. The 3-D version of (1) is

$$u_{xx} + u_{yy} + u_{zz} - au = f, \qquad x, y, z \in [-1, +1], \tag{7}$$

with boundary conditions of type (4) in each spatial direction. The solution of (7) is then approximated by the Tau method based on the 3-D Chebyshev series

$$u_{LMN} = \sum_{l=0}^{L} \sum_{m=0}^{M} \sum_{n=0}^{N} \tilde{u}_{l,m,n} T_l(x)\, T_m(y)\, T_n(z). \tag{8}$$

The full diagonalization technique performs the following steps:

(i) Preprocessing stage: computation of the 1-D B_x, B_y, B_z matrices of order $L-1$, $M-1$, $N-1$, respectively, and diagonalization of these matrices to produce the H_i, Λ_i eigenvector and eigenvalue matrices ($i = x, y, z$). In the $(L-1)$ $(M-1)$ $(N-1)$ space, the H_i and Λ_i matrices are proportional to the identity matrix in the other directions. The $(L-1)$ $(M-1)$ $(N-1)$ subsystem of (7) is then equivalent to

$$H_x H_y H_z (\Lambda_x + \Lambda_y + \Lambda_z - aI) H_z^{-1} H_y^{-1} H_x^{-1} \tilde{u} = D.$$

(ii) Computation of the modified source term D, applying (A.6), (A.9) in each spatial direction.

(iii) Scanning each spatial direction in succession, one applies the corresponding H_i^{-1} operator to the right-hand side to produce the source term of the full Helmholtz diagonal representation.

(iv) The solution is recovered, first, in the $(L-1)(M-1)(N-1)$ subspace, by successive applications of the H_i operators, and, finally, for the last components, by appropriate use of the boundary conditions.

In the partially diagonalized version of the algorithm, one must choose the direction in which matrix sustems are to be solved instead of using the diagonalization technique. The 3-D case is therefore solved by the same procedure as described in HZ, i.e., two diagonalizations are followed by the solution of matrix systems of quasi-tridiagonal type as noted by Gottlieb and Orszag [1]. These systems of order N, say, are solved in $0(8N)$ operations for Robbins boundary conditions. This operation count results essentially from the LU backsolving and the right-hand side calculation.

Table II presents the comparison of asymptotic operation counts for both algorithms in 2-D and 3-D cases.

TABLE II

Asymptotic Operation Counts for the Direct Spectral Solvers (Preprocessing Is Not Taken into Account and Coupling Is Assumed between Parities, i.e., Robbins-Type Boundary Conditions)

System size	HZ algorithm[a]	Full diagonalization
(L, M)	$2LM(4+M)$	$2LM(L+M)$
(L, M, N)	$2LMN(4+M+N)$	$2LMN(L+M+N)$

[a] The first direction (L) is solved and the others are diagonalized.

3. Pseudospectral Iterative Solver

The existence of highly developed packages for elliptic equations (Boisvert and Sweet [4]) within the finite difference (FD) context allows one to investigate the following interesting question: Is it possible to obtain spectral accuracy using an FD preconditioning? This question has been addressed by S. A. Orszag [5], who proposed an iterative scheme for linear and nonlinear equations. His theoretical analysis investigates the Fourier spectral schemes. In the present paper, the same kind of analysis is carried out for the Helmholtz equation within the Chebyshev spectral approximation. Let us recall the basic properties of the iterative scheme designed to solve $Lu = 0$, where L is a linear operator in this case. Let us call Lap the preconditioned FD operator built from centered differences at the Chebyshev collocation points. The correction $\delta u^{(n)}$ to some approximate solution $u^{(n)}$ at iteration n is obtained by

$$\delta u^{(n)} = -\,\mathrm{Lap}^{-1} L u^{(n)}, \tag{9a}$$

$$u^{(n+1)} = u^{(n)} + \alpha\, \delta u^{(n)}. \tag{9b}$$

An optimum value for the relaxation parameter α is given by $\alpha_{\mathrm{opt}} = 2/(M+m)$, where m and M are, respectively, the smallest and largest absolute eigenvalues of $\mathrm{Lap}^{-1}L$. Defining $\varepsilon^{(n)} = u - u^{(n)}$, the ratio $\|\varepsilon^{(n+1)}\|/\|\varepsilon^{(n)}\| = \|\delta u^{(n+1)}\|/\|\delta u^{(n)}\|$ is bounded by $r_{\mathrm{opt}} = (M-m)/(M+m)$. The problem reduces to finding the values of m and M for the Chebyshev Helmholtz operator.

In the case of d^2/dx^2, an analytical evaluation of m and M is presented in Appendix II. This calculation results in $m = 1$, $M \to \pi^2/4$ when the cutoff N of the Chebyshev series goes to infinity. For example, $M = 2.4$ for $N = 32$. For the 2-D Laplacian operator, the same results are obtained by numerical computation. For the Helmholtz operator, m remains 1 while M approaches the value of m as the Helmholtz parameter a (Eq. (1) or (7)) increases.

From these results, one may conclude that the Fourier analysis of the operator $\mathrm{Lap}^{-1}\, L$ provides a useful (and simple) tool to analyse the convergence behaviour of the iterative system. On the basis of these considerations, the conclusions of Orszag's analysis hold and throughout the iteration process it should be expected that $\|\varepsilon^{(16)}\| \leqslant 10^{-6}\,\|\varepsilon^{(0)}\|$ for $\alpha_{\mathrm{opt}} \simeq 4/7$.

In Orsag's algorithm, the iterative procedure uses the relaxation parameter fixed at its α_{opt} value, which is only asymptotically optimal. However, a better strategy can be achieved by considering that only a subset of a few relevant eigenvectors of the $\mathrm{Lap}^{-1}\, L$ operator is significant in the $\|\delta u^{(n)}\|$ reduction process. The span of this subset widens as the iterations proceed and at convergence the subset covers the whole eigenvector basis. Let us now denote by $m^{(n)}$, $M^{(n)}$ the subset of relevant eigenvalues at the nth iteration. Therefore, adjusting the relaxation parameter at each iteration to the subset $(m^{(n)}, M^{(n)})$, an accelerated procedure can be built.

As a conclusion of the above considerations, one can write the relation

$$\alpha_{\mathrm{opt}} \leqslant \alpha^{(n)} \leqslant 1,$$

and assuming that $\|\delta u^{(n)}\|/\|\delta u^{(n-1)}\|$ is a good estimate of $|1-\alpha^{(n)}M^{(n)}|$, then the next value of α results from

$$\alpha^{(n+1)} = \max\left(\alpha_{\text{opt}}, \frac{2}{M^{(n)}+1}\right). \tag{10}$$

The initial guess for α will always be $\alpha^{(0)} = 1$. In Eq. (10), $m^{(n)}$ has been set equal to 1 because, for elliptic equations, this choice does not noticeably influence the convergence rate of the iterative method.

Let us note that the proposed iterative procedure can be implemented without any a priori knowledge of the bound M of $\text{Lap}^{-1}L$. In particular, for Helmholtz operators, M lies in the range $[1, \pi^2/4]$ and its corresponding α_{opt} is greater than 4/7. Nevertheless, the application of (10) with $\alpha_{\text{opt}} = 4/7$ leads to a good convergence of the scheme without providing the M value.

How sensitive is the convergence rate to the nature of the boundary conditions? More specifically, does the presence of a first-order operator at the boundaries slow down the rate of convergence? To answer these questions, problem (1) was solved with Dirichlet or Neumann conditions, $\alpha^{\pm} = 1$, $\beta^{\pm} = 0$ or $\alpha^{\pm} = 0$, $\beta^{\pm} = 1$, respectively, in (2). The linear system for the correction δu is built up using centered FD. The right-hand side results from the spectral residue calculation for the PDE and the boundary conditions.

No significantly different behaviours appeared and excellent convergence rates were observed, i.e., $\varepsilon^{(16)} \simeq 10^{-10}\varepsilon^{(0)}$. Figure 1 shows the evolution of the maximum

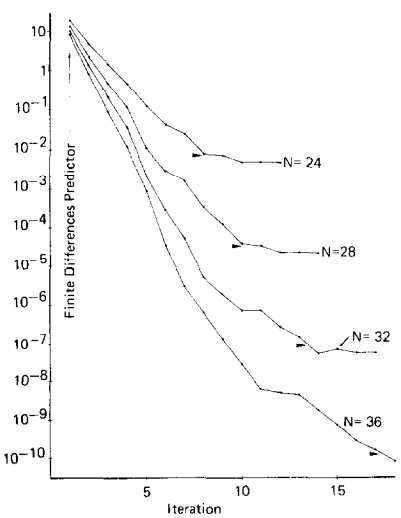

FIG. 1. Maximum residue $L_N u_N - f_N$ for Eq. (1) solved by the pseudospectral iterative solver with Neumann boundary conditions. The Helmholtz parameter a is 10^{-4}. The exact solution is $u = \sin 4\pi x + \cos 4\pi x$. In Figs. 1 to 3 the wedge indicates the spectral accuracy level achievable with a given spectral cutoff on the known analytical solution.

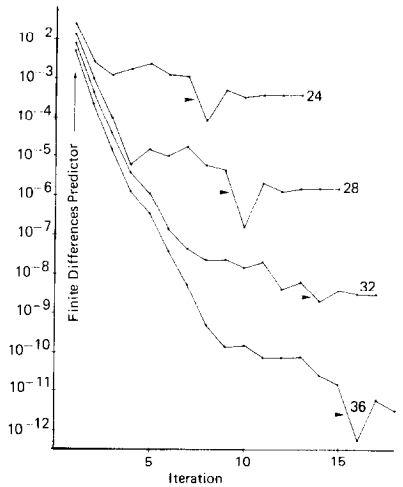

FIG. 2. Residue at $x=-1$ of the Neumann boundary condition from the 1-D Helmholtz pseudospectral iterative solver.

residue $L_N u_N - f_N$ of the PDE with respect to the iteration number for various Chebyshev cutoff values. Figure 2 shows the evolution of the residue of the left Neumann boundary condition. For both cases, the improvement over the FD prediction is quite striking and the spectral accuracy defined as the maximum residue for the analytical solution with a given spectral cutoff is obtained after a finite number of iterations.

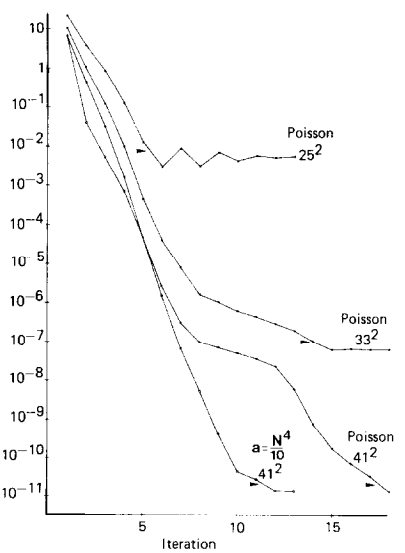

FIG. 3. Maximum residue for the 2-D pseudospectral iterative solver. The exact solution is $\sin 4\pi x \sin 4\pi y$.

TABLE III

Asymptotic Operation Counts Per Iteration for the Iterative Pseudospectral Solvers

System size	FD solver [7]	Discrete Chebyshev Transforms [9]
(L, M)	$3LM \text{ Log}_2 M$	$2LM \text{ Log}(LM)$
(L, M, N)	$3LMN \text{ Log}_2 M \text{ Log}_2 N$	$2LMN \text{ Log}(LMN)$

The same algorithm was applied to a 2-D version of the Helmholtz equation. The FD problem was solved by the BLKTRI routine from FISHPACK [6]. Figure 3 presents the evolution of the maximum spectral residue of the PDE for a 2-D problem. The same behaviour as in the 1-D case is observed.

The asymptotic operation count per iteration is given in Table III for 2-D and 3-D cases with the assumption that the FD solver performs cyclic reduction [7].

4. Comparative Evaluation of Both Algorithms

In Table IV, the execution times required by the direct spectral solvers are in good agreement with the asymptotic operation counts given in Table II. As expected, the full diagonalization solver is more expensive than the HZ algorithm; the difference between the two algorithms is proportionally smaller in the 3-D case than in the 2-D one. Nevertheless, the straightforward implementation of the fully vectorizable algorithm leads one to consider the HZ solver as well suited for large aspect ratio situations, where one cutoff value is much larger than the others.

TABLE IV

Execution Time in Seconds on a 3033 IBM Computer

System size	HZ algorithm	Full diagonalization solver	Ten iterations of pseudospectral solver		
			Total	FD solver	*DCT*
17^2	0.017	0.023	0.74	0.4	0.2
25^2	0.04	0.067	2.05	1.25	0.6
33^2	0.083	0.14	3.5	2.4	0.9
41^2	0.15	0.29[a]	6.1	4.4	1.7
49^2	0.23	0.47[a]			
9^3	0.03[a]	0.05			
17^3	0.35[a]	0.53			
25^3	1.51[a]	2.27			
33^3	4.35[a]	6.52			

[a] These times have been estimated from the asymptotic operation counts given in Table II.

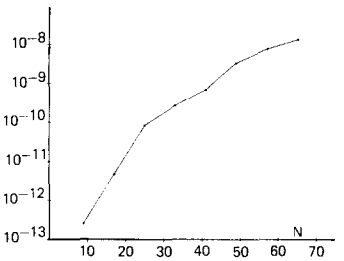

FIG. 4. Round-off errors for a 1-D diagonalization solver with Dirichlet boundary condition.

The computing time of the pseudospectral iterative solver is divided into two parts: 70% of the computation time is spent by the FD solver while the remaining 30% results from the Discrete Chebyshev Transforms [9].

Despite the fact that the pseudospectral approach is more expensive in terms of computer time compared to the fast direct solver for the Helmholtz equation, its range of applications is much wider. The pseudospectral algorithm is valid for general elliptic boundary value problems with linear or nonlinear conditions. The limitations (if any) arise from the existing facilities to solve the preconditioned problem and their ability to work with a Chebyshev collocation grid.

The spectral accuracy, i.e., the maximum residue $L_N u_N - f_N$ one would obtain from the known solution described with, say, $N+1$ Chebyshev polynomials, will be achieved by the pseudospectral iterative scheme, whatever the solution smoothness or the spectral cutoff. Of course these two parameters do monitor the spectral accuracy level. Also, the number of iterations needed to achieve spectral accuracy will depend on the spatial structure of the solution field. The more complicated it is, the more iterations will be necessary. Nevertheless, the worst rate of convergence would still be that obtained with Orszag's relaxation factor. On the other hand the direct spectral solver is subject to some inaccuracy as already mentioned by HZ [2] due to the preprocessing calculation of eigenvalues and eigenvectors. Figure 4 displays the round-off error evolution with respect to the cutoff N for the 1-D problem (1) with Dirichlet conditions. Here the preprocessing is calculated using 64-bit words. When N goes from 8 to 64, almost five significant digits are lost. For a reasonable cost of preprocessing, this kind of numerical error prohibits the use of the direct solver for large N values.

GENERAL CONCLUSIONS

Up to $N = 50$ (say), the Helmholtz equation with linear boundary conditions can be solved quite efficiently by the full diagonalization technique which is the easiest algorithm to implement and the best one for vectorization. However, if one of the cutoff values is greater than the others, the partial diagonalization in the directions

corresponding to the low cutoffs constitutes the best algorithmic choice. For more general elliptic operators, the pseudospectral scheme appears to be well suited although the iterative character of the algorithm leads to time-consuming procedures.

APPENDIX I

Referring to the Poisson 1-D problem presented in Section 2, we are faced with the following linear system (Eqs. (3)–(4)):

$$\frac{1}{c_n} \sum_{\substack{p=n+2 \\ p+n \text{ even}}}^{N} p(p^2-n^2)\,\tilde{u}_p - a\tilde{u}_n = f_n, \qquad 0 \leqslant n \leqslant N-2, \tag{A.1}$$

$$\sum_{n=0}^{N} (\pm 1)^n \left[\alpha_\pm \pm \beta_\pm n^2\right] \tilde{u}_n = g_\pm, \tag{A.2}$$

where $c_0 = 2$ and $c_i = 1$, $\forall i > 0$. The elimination of $\tilde{u}_N$, $\tilde{u}_{N-1}$ between (A.1) and (A.2) proceeds as follows. First, let us evaluate $\tilde{u}_N$ and $\tilde{u}_{N-1}$ from the two equations (A.2). We obtain, with the following auxiliary quantities:

$$\begin{aligned}
A_-(n) &= \alpha_- - \beta_- n^2, \\
A_+(n) &= \alpha_+ + \beta_+ n^2, \\
Den &= -A_+(N) A_-(N-1) - A_-(N) A_+(N-1), \\
\tilde{u}_{N-1} &= \Bigg[g_- A_+(N) - g_+ A_-(N) - \sum_{n=0}^{N-2} (A_+(N)(-1)^n A_-(n) \\
&\qquad - A_-(N) A_+(n))\,\tilde{u}_n \Bigg] \Big/ Den,
\end{aligned} \tag{A.3}$$

$$\begin{aligned}
\tilde{u}_N &= \Bigg[g_+ A_-(N-1) + g_- A_+(N-1) + \sum_{n=0}^{N-2} (A_-(N-1) A_+(n) \\
&\qquad + (-1)^n A_-(n) A_+(N-1))\,\tilde{u}_n \Bigg] \Big/ Den.
\end{aligned} \tag{A.4}$$

Substituting (A.3)–(A.4) into (A.1), the $(N-1)^2$ system can be written as

$$(B_x - aI)\,\tilde{u} = D, \tag{A.5}$$

where I is the unit matrix of order $N-1$. The B_x matrix translates, in the Chebyshev space, the $\partial^2/\partial x^2$ operator together with the general homogeneous linear boundary conditions (LHS of (A.2)). The B_x and D matrices are formed from the elements:

(i) *Even n*

$$D_n = f_n - \frac{1}{c_n}\frac{N(N^2-n^2)}{Den}\,(g_+ A_-(N-1) + g_- A_+(N-1)), \qquad 0 \leqslant n \leqslant N-2. \quad \text{(A.6)}$$

For every p such that $0 \leqslant p \leqslant n+1$ and for odd values of p such that $n+3 \leqslant p \leqslant N-2$, we have

$$B_{np} = \frac{1}{c_n}\frac{N(N^2-n^2)}{Den}\,(A_-(N-1)\,A_+(p) + (-1)^p A_-(p)\,A_+(N-1)). \quad \text{(A.7)}$$

For every even p such that $n+2 \leqslant p \leqslant N-2$

$$B_{np} = \frac{1}{c_n}\,p(p^2-n^2) + \text{(A.7)}. \quad \text{(A.8)}$$

(ii) *Odd n*

$$D_n = f_N + \frac{1}{c_n}\frac{(N-1)}{Den}\,((N-1)^2-n^2)(g_- A_+(N) - g_+ A_-(N)). \quad \text{(A.9)}$$

For every p such that $0 \leqslant p \leqslant n+1$ and even p such that $n+3 \leqslant p \leqslant N-2$,

$$B_{np} = -\frac{1}{c_n}\frac{(N-1)}{Den}\,((N-1)^2-n^2)(A_+(N)(-1)^p A_-(p) - A_-(N)\,A_+(p)). \quad \text{(A.10)}$$

For every odd p such that $n+2 \leqslant p \leqslant N-3$

$$B_{np} = \frac{1}{c_n}\,p(p^2-n^2) + \text{(A.10)}. \quad \text{(A.11)}$$

Appendix II

We wish to evaluate the lowest and largest absolute eigenvalues of $\text{Lap}^{-1} L$, where L is the Chebyshev representation of $\partial^2/\partial x^2$, while Lap is the centered finite difference approximation based on the Chebyshev collocation points

$$x_i = \cos\theta_i, \qquad \theta_i = i\pi/N, \qquad i = 1,\ldots, N-1.$$

For that purpose, let us show that $\text{Lap}^{-1} L$ has a triangular form in the Chebyshev coefficient space.

Using the notations

$$u_N(x_i) = \sum_{n=0}^{N} \tilde{u}_n T_n(x_i), \tag{A.12}$$

$$Lu_n(x_i) = \sum_{n=0}^{N} \tilde{u}_n^{(2)} T_n(x_i), \tag{A.13}$$

$$\text{Lap}\, u_N(x_i) = \sum_{n=0}^{N} \tilde{u}_n^{(\hat{2})} T_n(x_i), \tag{A.14}$$

the $\tilde{u}_n^{(2)}$ are well known (see [1], for example), while $\tilde{u}_n^{(\hat{2})}$ will result from the present development.

The application of the standard 3-point finite difference to $T_n(x_i)$,

$$\text{Lap}[T_n(x_i)] = \frac{T_n(x_{i-1})}{a_i} + \frac{T_n(x_i)}{b_i} + \frac{T_n(x_{i+1})}{c_i}, \tag{A.15}$$

leads to the calculation of a_i, b_i, c_i, which are the coefficients corresponding to the nonuniform Chebyshev collocation grid, namely,

$$\begin{aligned} a_i &= 4 \sin^2 \frac{\pi}{2N} \sin\left(\theta_i + \frac{\pi}{2N}\right) \sin\theta_i \cos\frac{\pi}{2N}, \\ b_i &= 2 \sin^2 \frac{\pi}{2N} \sin\left(\theta_i + \frac{\pi}{2N}\right) \sin\left(\theta_i - \frac{\pi}{2N}\right), \\ c_i &= 4 \sin^2 \frac{\pi}{2N} \sin\left(\theta_i - \frac{\pi}{2N}\right) \sin\theta_i \cos\frac{\pi}{2N}. \end{aligned} \tag{A.16}$$

Using Chebyshev classical formulae (see Rivlin [8]), it is easy to show that

$$\begin{aligned} \text{Lap}(T_n(x_i)) = &\frac{4 \sin n \dfrac{\pi}{2N}}{\sin^3 \dfrac{\pi}{2N} \cos \dfrac{\pi}{2N}} \cdot \sum_{p=0}^{[(n-2)/2]} \frac{\sin(n-1-p)\dfrac{\pi}{2N} \sin(p+1)\dfrac{\pi}{2N}}{c_{n-2-2p}} \\ &\times T_{n-2-2p}(x_i), \end{aligned} \tag{A.17}$$

where [ ] denotes the integral part of the quantity.

Combining Eqs. (A.12), (A.17), one obtains (A.14) where the $\tilde{u}_n^{(\hat{2})}$ coefficients are

$$\tilde{u}_n^{(\hat{2})} = \frac{1}{c_n} \sum_{\substack{p=n+2 \\ p+n \text{ even}}}^{N} \frac{4 \sin p \dfrac{\pi}{2N} \sin\left(\dfrac{p+n}{2}\right)\dfrac{\pi}{2N} \sin\left(\dfrac{p-n}{2}\right)\dfrac{\pi}{2N}}{\sin^3 \dfrac{\pi}{2N} \cos\dfrac{\pi}{2N}} \cdot \tilde{u}_p. \tag{A.18}$$

For fixed p and n, the coefficients appearing in (A.18) when $N \to \infty$ approach $4p((p+n)/2)((p-n)/2)$, i.e., the coefficients of the $\tilde{u}_n^{(2)}$. Following the well-known

tridiagonal relation between $\tilde{u}_n$ and $\tilde{u}_n^{(2)}$, it is easy to derive a similar relation between $\tilde{u}_n$ and $\tilde{u}_n^{(\hat{2})}$.

$$\tilde{u}_n = \alpha_n \tilde{u}_{n-2}^{(\hat{2})} + \beta_n \tilde{u}_n^{(\hat{2})} + \gamma_n \tilde{u}_{n+2}^{(\hat{2})}, \qquad n \geqslant 2, \tag{A.19}$$

where

$$\alpha_n = \frac{\sin^2 \frac{\pi}{2N} \cdot \cos \frac{\pi}{2N} \cdot c_{n-2}}{4 \cdot \sin(n-1)\frac{\pi}{2N} \cdot \sin n \frac{\pi}{2N}},$$

$$\beta_n = \frac{-\sin^2 \frac{\pi}{2N} \cdot \cos^2 \frac{\pi}{2N}}{2 \cdot \sin(n+1)\frac{\pi}{2N} \cdot \sin(n-1)\frac{\pi}{2N}}, \tag{A.20}$$

$$\gamma_n = \frac{\sin^2 \frac{\pi}{2N} \cdot \cos \frac{\pi}{2N}}{4 \cdot \sin(n+1)\frac{\pi}{2N} \cdot \sin n \frac{\pi}{2N}}.$$

Thus, combining (A.13) and (A.19), we finally obtain

$$\mathrm{Lap}^{-1} \cdot L(u_N(x_i)) = \sum_{n=0}^{N} (\mathscr{E}_{np} \tilde{u}_p)\, T_n(x_i), \tag{A.21}$$

where $\mathscr{E}$ is an upper triangular matrix, defined as

$$\mathscr{E}_{np}\tilde{u}_p = \frac{n(n-1)\sin^2 \frac{\pi}{2N} \cos \frac{\pi}{2N}}{\sin(n-1)\frac{\pi}{2N} \sin \frac{n\pi}{2N}} \tilde{u}_n + \frac{\sin^2 \frac{\pi}{2N} \cos \frac{\pi}{2N}}{\sin n \frac{\pi}{2N}}$$

$$\times \left[\frac{n-1}{\sin(n-1)\frac{\pi}{2N}} - \frac{n+1}{\sin(n+1)\frac{\pi}{2N}} \right] \sum_{\substack{p=n+2 \\ p+n \text{ even}}}^{N} p\tilde{u}_p, \qquad n \geqslant 2. \tag{A.22}$$

By inspection of (A.22), one obtains the $N-1$ eigenvalues:

$$\frac{n(n-1)\sin^2 \frac{\pi}{2N} \cos \frac{\pi}{2N}}{\sin n \frac{\pi}{2N} \cdot \sin(n-1)\frac{\pi}{2N}}, \qquad 2 \leqslant n \leqslant N.$$

This set of eigenvalues is obviously bounded by 1 and $\pi^2/4$.

ACKNOWLEDGMENT

This work has been done under CNRS-PIRSEM Contract App 1067, for the Marseille team.

REFERENCES

1. D. GOTTLIEB AND S. A. ORSZAG, "Numerical Analysis of Spectral Methods: Theory and Applications," SIAM monograph No. 26, Philadelphia, Penn., 1977.
2. D. B. HAIDVOGEL AND T. ZANG, The accurate solution of Poisson's equation by expansion in Chebyshev polynomials, *J. Comput. Phys.* **30** (1979), 167–180.
3. D. GOTTLIEB AND L. LUSTMAN, "The Spectrum of the Chebyshev Collocation Operator for the Heat Equation," Icase Report No. 82–12, ICASE, Hampton, Va.
4. R. A. SWEET AND R. F. BOISVERT, A survey of mathematical software for elliptic boundary value problems, *in* "Proceedings, 10th IMACS on System Simulation and Scientific Computation, Montreal, Canada, 1982," pp. 449–451.
5. S. A. ORSZAG, Spectral methods for problems in complex geometries, *in* "Numerical Methods for Partial Differential Equations" (S. V. Parter, Ed.), Academic Press, New York, 1979.
6. J. ADAMS, P. SWARZTRAUBER, AND R. SWEET, "FISHBACK, a Package of Fortran Subprograms for the Solution of Separable Elliptic Partial Differential Equations," NCAR, Boulder, Colo.
7. P. SWARZTRAUBER, A direct method for the discrete solution of separable elliptic equations, *SIAM J. Numer. Anal.* **11** (1974), 1136–1150.
8. T. J. RIVLIN, "The Chebyshev Polynomials," Wiley, New York, 1974.
9. M. DEVILLE AND G. LABROSSE, An algorithm for the evaluation of multidimensional (direct and inverse) discrete Chebyshev transforms, *J. Comput. Appl. Math* **8** (4) (1982), 293–304.